Datasheet for 600-401-886

Beta Actin Antibody

Overview

Description:	Anti-Beta Actin (RABBIT) Antibody - 600-401-886
Item No.:	600-401-886
Size:	200 µg
Applications:	ELISA, IF, WB
Reactivity:	Human, Mouse, Leopard Frog
Host Species:	Rabbit

Product Details

Background:	In vertebrates 3 main groups of actin isoforms, alpha, beta and gamma have been identified. Alpha actins are found in muscle tissues and are a major constituent of the contractile apparatus. Beta and gamma actins coexist in most cell types as components of the cyto-skeleton and as mediators of internal cell motility. Beta actins are highly conserved proteins that are involved in cell motility, structure and integrity. Beta actins are cytoplasmic proteins. Anti-Actin is a loading control antibody and is critical for the correct interpretation of your western blot. Beta-Actin Loading Control Antibody is used to normalize the levels of protein detected by confirming that protein loading is uniform across the gel.
Synonyms:	rabbit anti-beta Actin Antibody, Actin Antibody, Loading Control Antibody, beta actin, ß actin, anti-beta actin antibody
Host Species:	Rabbit
Clonality:	Polyclonal
Format:	IgG

Target Details

Gene Name:	ACTB
Reactivity:	Human, Mouse, Leopard Frog
Immunogen Type:	Conjugated Peptide

Immunogen:	beta-Actin Loading Control Antibody was prepared from whole rabbit serum produced by repeated immunizations with a synthetic peptide corresponding to C-Terminal region near amino acids 350-375 of Human beta Actin.
Purity/Specificity:	Anti-beta-Actin Loading Control Antibody reacts with Human, Rat, Monkey and Mouse. beta-Actin Loading Control Antibody is expected to cross-react with a wide range of species due to sequence homology. Anti-Beta Actin is affinity-purified antibody is directed against human beta Actin protein. A BLAST analysis was used to suggest that this antibody would react with beta Actin from a wide range of organisms, including most vertebrates and some yeast. Broad reactivity makes this antibody an excellent loading control.
Relevant Links:	• GeneID - • NCBI - NP_001092.1 • UniProtKB - P60709

Application Details

Tested Applications:	ELISA, IF, WB
Application Note:	Anti-beta Actin Antibody has been tested for use in ELISA, immunofluorescence, and western blot. Specific conditions for reactivity should be optimized by the end user. Beta actin present in fibroblast connective tissue stains very brightly. Beta actin present in neuromuscular junctions also stains. Paraformaldehyde fixation yields brighter staining than formalin or methanol fixation. Expect a band at ~42 kDa in size corresponding to beta actin by western blotting in the appropriate cell lysate or extract.
Assay Dilutions:	All assays should be optimized by the user. Recommended dilutions (if any) may be listed below.
ELISA:	1:10,000 - 1:40,000
IF:	1:500 - 1:2,000
WB:	1:1,000 - 1:4,000

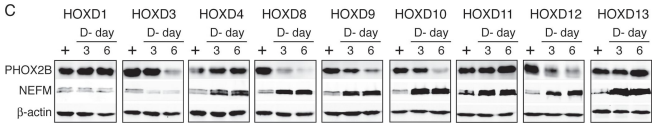
Formulation

Physical State:	Liquid (sterile filtered)
Concentration:	1.0 mg/mL by UV absorbance at 280 nm
Buffer:	0.02 M Potassium Phosphate, 0.15 M Sodium Chloride, pH 7.2
Preservative:	0.01% (w/v) Sodium Azide
Stabilizer:	None

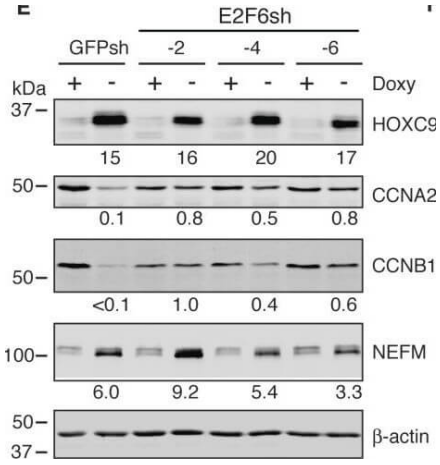
Shipping & Handling

Shipping Condition:	Dry Ice
Storage Condition:	Store beta-Actin Loading Control Antibody at -20° C prior to opening. Aliquot contents and freeze at -20° C or below for extended storage. Avoid cycles of freezing and thawing. Centrifuge product if not completely clear after standing at room temperature. This product is stable for several weeks at 4° C as an undiluted liquid. Dilute only prior to immediate use.
Expiration:	Expiration date is one (1) year from date of receipt.

Images

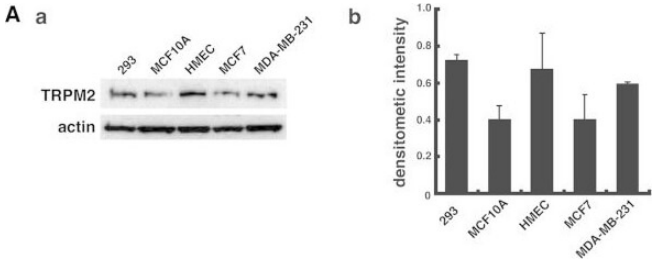


Western Blot
Distinct functions of HOXD proteins in regulation of neuronal differentiation.(A–B) Phase contrast imaging (A) and NEFM immunofluorescent staining (B) of BE(2)-C/Tet-Off/myc-HOXD cells cultured in the presence or absence of Doxy for 7 days. Scale bars, 50 µm. Shown are representative of three independent experiments with similar results. (C) Immunoblot analysis of PHOX2B and NEFM protein levels in the same cell samples described in Figure 3. Beta-actin levels are shown as loading control. Shown are representative of two independent experiments with similar results. (D) Quantification of NEFM mRNA levels in BE(2)-C/Tet-Off/myc-HOXD cells cultured in the presence or absence of Doxy for 3 days. The NEFM mRNA levels in BE(2)-C/Tet-Off/myc-HOXD cells in the presence of Doxy were designated as 1.0 (dashed line). The data were from two independent samples with each being assayed in triplicates and analyzed using two-tailed Student's t-test with the p values indicated. Error bars, SD. Figure provided by CiteAb. Source: PLoS One, PMID: 22879880.



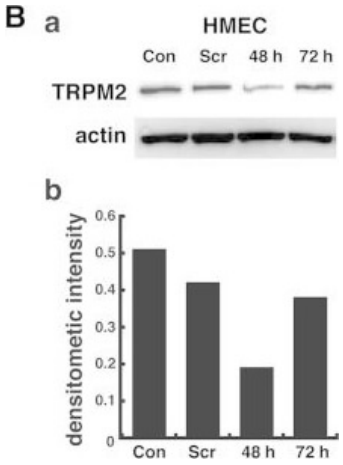
Western Blot

E2F6 is essential for HOXC9 induction of G1 arrest and repression of cell cycle genes. (A) Immunoblot analysis of E2F6 levels in BE(2)-C/Tet-Off/myc-HOXC9 cells infected with lentiviruses expressing shRNA against GFP or various coding regions of E2F6. E2F6 levels were quantified against β-actin. (B-D) Phase contrast imaging and growth assay (B) and cell cycle analysis (C, D) showing E2F6 knockdown abrogated HOXC9-induced growth arrest. Error bars, SD (n = 4). (E-F) Immunoblot analysis (E) and quantification (F) showing that E2F6 knockdown abrogated HOXC9 repression of cyclins, but not HOXC9 induction of NEFM. HOXC9, CCNA2, CCNB1 and NEFM levels were quantified against β-actin with the protein levels in GFPsh-expressing cells cultured in the presence of doxycycline (Doxy+) were defined as 1.0 (dashed lines). Error bars, SD (n = 3). Data in (D) and (F) were analyzed with unpaired, two-tailed Student's t-test and p values are indicated. Figure provided by CiteAb. Source: BMC Genomics, PMID: 24274069.

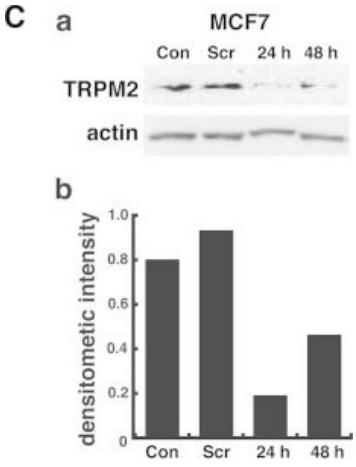


Western Blot

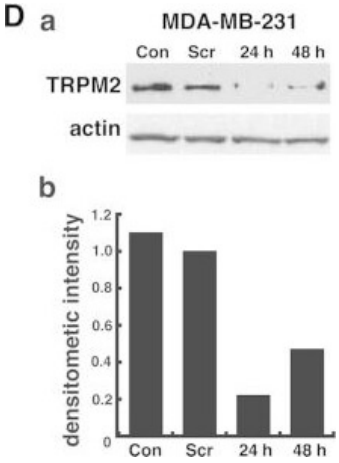
TRPM2 levels in breast cell lines and knockdown of TRPM2 levels by RNAi silencing. (A) Immunoblot (a) and densitometric quantification (b) of TRPM2 protein levels in two noncancerous breast cell lines (HMEC, MCF-10A) and two cancerous breast cell lines (MCF-7, MDA-MB-231). Immunoblot detection of TRPM2 protein levels in human embryonic kidney cells (HEK 293) provided the positive control. (B) RNAi silencing of TRPM2 in noncancerous HMEC cells (a), and quantification of protein levels by densitometry (b). (C and D) RNAi silencing of TRPM2 in MCF-7 and MDA-MB-231 breast adenocarcinoma cells (a) and quantification of protein levels by densitometry (b). All densitometric values represent TRPM2:actin ratios. Con, untreated negative control cells; Scr, treatment with scrambled negative control siRNA oligos. Figure provided by CiteAb. Source: Int J Oncol, PMID: 25760245.



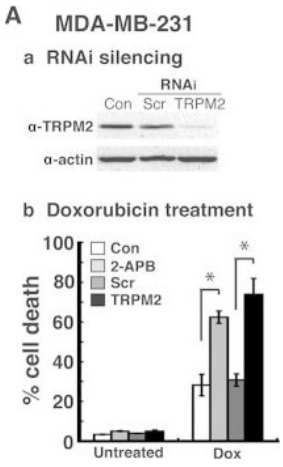
Western Blot
TRPM2 levels in breast cell lines and knockdown of TRPM2 levels by RNAi silencing. (A) Immunoblot (a) and densitometric quantification (b) of TRPM2 protein levels in two noncancerous breast cell lines (HMEC, MCF-10A) and two cancerous breast cell lines (MCF-7, MDA-MB-231). Immunoblot detection of TRPM2 protein levels in human embryonic kidney cells (HEK 293) provided the positive control. (B) RNAi silencing of TRPM2 in noncancerous HMEC cells (a), and quantification of protein levels by densitometry (b). (C and D) RNAi silencing of TRPM2 in MCF-7 and MDA-MB-231 breast adenocarcinoma cells (a) and quantification of protein levels by densitometry (b). All densitometric values represent TRPM2:actin ratios. Con, untreated negative control cells; Scr, treatment with scrambled negative control siRNA oligos. Figure provided by CiteAb.
Source: Int J Oncol, PMID: 25760245.



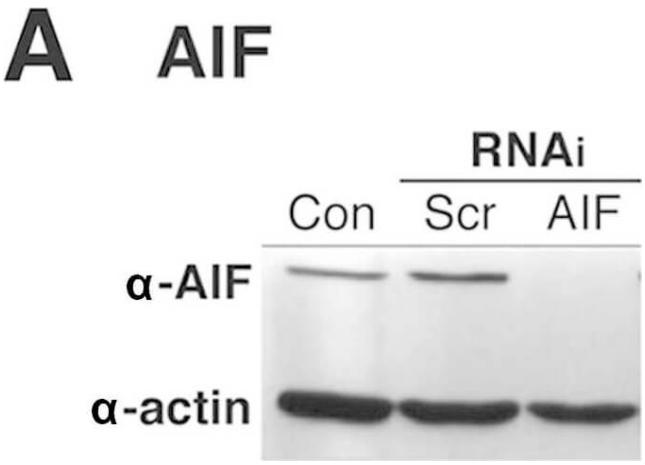
Western Blot
TRPM2 levels in breast cell lines and knockdown of TRPM2 levels by RNAi silencing. (A) Immunoblot (a) and densitometric quantification (b) of TRPM2 protein levels in two noncancerous breast cell lines (HMEC, MCF-10A) and two cancerous breast cell lines (MCF-7, MDA-MB-231). Immunoblot detection of TRPM2 protein levels in human embryonic kidney cells (HEK 293) provided the positive control. (B) RNAi silencing of TRPM2 in noncancerous HMEC cells (a), and quantification of protein levels by densitometry (b). (C and D) RNAi silencing of TRPM2 in MCF-7 and MDA-MB-231 breast adenocarcinoma cells (a) and quantification of protein levels by densitometry (b). All densitometric values represent TRPM2:actin ratios. Con, untreated negative control cells; Scr, treatment with scrambled negative control siRNA oligos. Figure provided by CiteAb.
Source: Int J Oncol, PMID: 25760245.



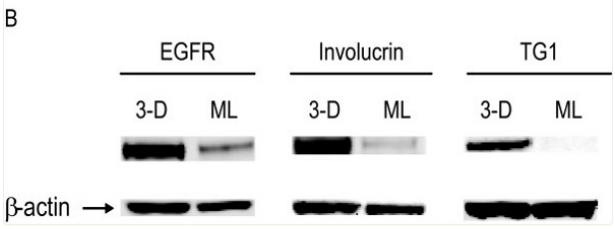
Western Blot
TRPM2 levels in breast cell lines and knockdown of TRPM2 levels by RNAi silencing. (A) Immunoblot (a) and densitometric quantification (b) of TRPM2 protein levels in two noncancerous breast cell lines (HMEC, MCF-10A) and two cancerous breast cell lines (MCF-7, MDA-MB-231). Immunoblot detection of TRPM2 protein levels in human embryonic kidney cells (HEK 293) provided the positive control. (B) RNAi silencing of TRPM2 in noncancerous HMEC cells (a), and quantification of protein levels by densitometry (b). (C and D) RNAi silencing of TRPM2 in MCF-7 and MDA-MB-231 breast adenocarcinoma cells (a) and quantification of protein levels by densitometry (b). All densitometric values represent TRPM2:actin ratios. Con, untreated negative control cells; Scr, treatment with scrambled negative control siRNA oligos. Figure provided by CiteAb. Source: Int J Oncol, PMID: 25760245.



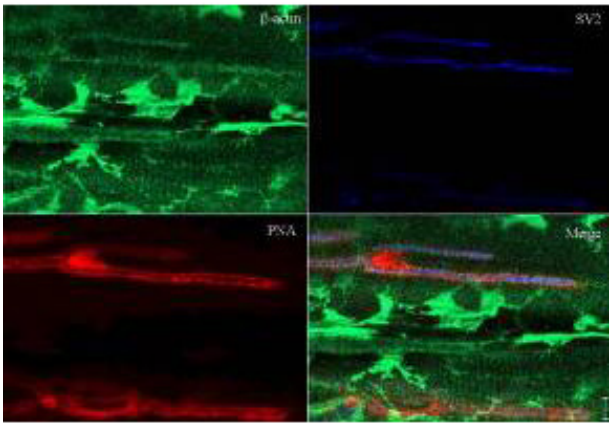
Western Blot
Effects of TRPM2 inhibition and RNAi knockdown in cancerous and non-cancerous breast cell lines after chemotherapeutic treatments. Immunoblot levels of TRPM2 protein after TRPM2 RNAi silencing (a) and quantification of cell death by flow cytometry (b) in (A) MDA-MB-231 breast adenocarcinoma, (B) MCF-7 breast adenocarcinoma and (C) human mammary epithelial cells (HMECs), a non-cancerous primary breast cell line. For RNAi silencing, cells were transfected with 100 nM anti-TRPM2 duplex siRNA oligos (TRPM2) or 100 nM negative control scrambled duplex siRNA oligos (Scr). Loading controls for immunoblots were provided by the immunodetection of β-actin. For chemotherapeutic treatments, the cells were pretreated 30 min with the TRPM2 inhibitor, 2-APB, and then subsequently treated with (A-b) 2 µM doxorubicin (Dox) until analysis; (B-b) 7 µM tamoxifen (Tam) until analysis; and (C-b) 2 µM doxorubicin (Dox) until analysis. Con, untransfected negative control cells. All error bars represent the SEM. *p<0.05 via one-way ANOVA and unpaired Student's t-test. Figure provided by CiteAb. Source: Oncol Rep, PMID: 26178079.



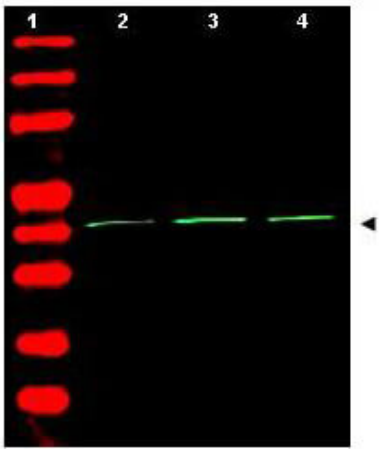
Western Blot
Analysis of poly(ADP-ribose)-mediated caspase-independent cell death in breast adenocarcinoma cells after TRPM2 inhibition and chemotherapeutic treatments. Immunoblot detection of (A) apoptosis-inducing factor (AIF) and (B) poly (ADP-ribose) glycohydrolase (PARG) in MDA-MB-231 breast adenocarcinoma cells after RNAi silencing. Loading controls for immunoblots were provided by the immunodetection of β-actin. Con, untransfected cells; Scr, cells transfected with negative control scrambled siRNA oligos. (C) Quantification of cell death by flow cytometry was performed in MDA-MB-231 cells after RNAi knockdown of AIF or PARG, pretreatment with 20 µM ACA for 30 min and treatment with 100 µM MNNG. *p<0.05, one-way ANOVA and unpaired Student's t-test; error bars represent the SEM. Figure provided by CiteAb. Source: Oncol Rep, PMID: 26178079.



Western Blot
Expression of corneal epithelial gene markers. (B) The relative protein expression levels of EGFR (p/n 100-401-149), involucrin and TG1 as determined by Western blot assay; β-actin (p/n 600-401-886) was used as a loading control. Fig 3. PMID: 19638217



Immunohistochemistry
Immunohistochemistry of Rabbit Anti-Beta Actin Antibody. Tissue: sections 4.2 mm thick of rana pipiens tissue. Fixation: formalin fixed paraffin embedded. Antigen retrieval: not required. Primary antibody: Beta Actin antibody at 1:200 for 1 h at RT. Secondary antibody: Peroxidase rabbit secondary antibody at 1:10,000 for 45 min at RT. Localization: Beta Actin is at the neuromuscular junction. Staining: Beta Actin as precipitated green signal with red and blue counterstain.



Western Blot
Western Blot of Rabbit Anti-Beta Actin Antibody. Lane 1: molecular weight. Lane 2: human embryonic kidney 293 (p/n W09-000-365). Lane 3: human lung carcinoma A549 (p/n W09-001-372). Lane 4: mouse brain (p/n W10-000-T004). Load: 35 µg per lane. Primary antibody: Beta Actin antibody at 1:1,500 for overnight at 4°C. Secondary antibody: IRDye800™ rabbit secondary antibody at 1:10,000 for 45 min at RT. Block: 5% BLOTTO (p/n B501-0500) overnight at 4°C. Predicted/Observed size: ~42 kDa corresponding to beta Actin (arrowhead). Other band(s): none.

References

- Freiría-Martínez L et al. Selective Antiproliferative Effects of Marine Oils on Neuroblastoma Cells in 3D Cultures. *Mar Drugs.* (2025)
- Low R et al. Prolonged Inhibition of the MEK1/2-ERK Signaling Axis Primes Interleukin-1 Beta Expression through Histone 3 Lysine 9 Demethylation in Murine Macrophages. *Int J Mol Sci.* (2023)
- McKamey SG et al. Antagonism of the transient receptor potential melastatin2 channel leads to targeted antitumor effects in primary human malignant melanoma cells. *Int J Oncol.* (2022)
- Hildebrandt J et al. Pro-inflammatory activation changes intracellular transport of bevacizumab in the retinal pigment epithelium in vitro. *Graefes Arch Clin Exp Ophthalmol.* (2022)
- Ogi K et al. ORMDL3 overexpression facilitates FcεRI-mediated transcription of proinflammatory cytokines and thapsigargin-mediated PERK phosphorylation in RBL-2H3 cells. *Immun Inflamm Dis.* (2021)
- Rodrigues-Amorim D et al. The Role of the Second Extracellular Loop of Norepinephrine Transporter, Neurotrophin-3 and Tropomyosin Receptor Kinase C in T Cells: A Peripheral Biomarker in the Etiology of Schizophrenia. *Int J Mol Sci.* (2021)
- Ilic N et al. SMURF2-mediated ubiquitin signaling plays an essential role in the regulation of PARP1 PARylating activity, molecular interactions, and functions in mammalian cells. *FASEB J.* (2021)
- Rosas-Ballina M. et al. Classical Activation of Macrophages Leads to Lipid Droplet Formation Without de novo Fatty Acid Synthesis. *Front Immunol.* (2020)
- Tatomir A et al. RGC-32 Regulates Generation of Reactive Astrocytes in Experimental Autoimmune Encephalomyelitis. *Frontiers in Immunology* (2020)
- D'Souza M et al. Regulator of G-protein signaling 5 protein protects against anxiety-and depression-like behavior. *Behav Pharmacol.* (2019)
- Coleman et al. Cathepsin B plays a key role in optimal production of the influenza A virus. *Journal of Virology & Antiviral Research* (2018)

- Borroni et al. Smurf2 regulates stability and the autophagic-lysosomal turnover of lamin A and its disease-associated form progerin. *Aging Cell* (2018)
- Olive et al. Accounting for tumor heterogeneity when using CRISPR-Cas9 for cancer progression and drug sensitivity studies. *PLOS One* (2018)
- Dai J et al. Intracellular BH3 Profiling Reveals Shifts in Antiapoptotic Dependency in Human B Cell Maturation and Mitogen-Stimulated Proliferation. *J Immunol.* (2018)
- Gillis NE et al. Thyroid Hormone Receptor β Suppression of RUNX2 Is Mediated by Brahma-Related Gene 1–Dependent Chromatin Remodeling. *Endocrinology.* (2018)
- Schanze N et al. 3-Iodothyronamine decreases expression of genes involved in iodide metabolism in mouse thyroids and inhibits iodide uptake in PCCL3 thyrocytes. *Thyroid.* (2017)
- Chen et al. Increased B7-H4 expression during esophageal squamous cell carcinogenesis is associated with IL-6/STAT3 signaling pathway activation in mice. *Oncology Letters* (2017)
- Lodola et al. VEGF-induced intracellular Ca2+ oscillations are down-regulated and do not stimulate angiogenesis in breast cancer-derived endothelial colony forming cells. *Oncotarget* (2017)
- Heaton BE et al. A CRISPR Activation Screen Identifies a Pan-avian Influenza Virus Inhibitory Host Factor. *Cell Rep.* (2017)
- McFadden K et al. Metabolic stress is a barrier to Epstein-Barr virus-mediated B-cell immortalization. *Proc Natl Acad Sci USA.* (2016)
- Liu M et al. Transcriptional Profiling Reveals a Common Metabolic Program in High-Risk Human Neuroblastoma and Mouse Neuroblastoma Sphere-Forming Cells. *Cell Rep.* (2016)
- Zhao E et al. KDM4C and ATF4 Cooperate in Transcriptional Control of Amino Acid Metabolism. *Cell Rep.* (2016)
- Campos et al. Alix-mediated assembly of the actomyosin-tight junction polarity complex preserves epithelial polarity and epithelial barrier. *Nature Communications* (2016)
- Zuccolo E et al. Constitutive Store-Operated Ca(2+) Entry Leads to Enhanced Nitric Oxide Production and Proliferation in Infantile Hemangioma-Derived Endothelial Colony-Forming Cells. *Stem Cells Dev.* (2016)
- Carr FE et al. Thyroid hormone receptor-β (TRβ) mediates runt-related transcription factor 2 (Runx2) expression in thyroid cancer cells: A novel signaling pathway in thyroid cancer. *Endocrinology.* (2016)
- Hopkins et al. Inhibition of the transient receptor potential melastatin-2 channel causes increased DNA damage and decreased proliferation in breast adenocarcinoma cells. *International Journal of Oncology* (2015)
- Koh et al. Enhanced cytotoxicity in triple-negative and estrogen receptor□positive breast adenocarcinoma cells due to inhibition of the transient receptor potential melastatin-2 channel. *Oncology Reports* (2015)
- Rae et al. A novel retroviral mutagenesis screen identifies prognostic genes in RUNX1 mediated myeloid leukemogenesis. *Oncotarget* (2015)
- Maragkoudaki et al. Specific detection of OCT4 isoforms in inflammatory bowel disease. *Gut Pathogens* (2015)
- Papaconstantinou I et al. Effect of infliximab on the healing of intestinal anastomosis. An experimental study in rats. *Int J Surg.* (2014)
- Dragoni S et al. Store-operated Ca2+ entry does not control proliferation in primary cultures of human metastatic renal cellular carcinoma. *Biomed Res Int.* (2014)

- Zha Y et al. MEIS2 is essential for neuroblastoma cell survival and proliferation by transcriptional control of M-phase progression. *Cell Death Dis.* (2014)
- Dragoni S et al. Enhanced expression of Stim, Orai, and TRPC transcripts and proteins in endothelial progenitor cells isolated from patients with primary myelofibrosis. *PLoS One.* (2014)
- View More ...

Disclaimer

This product is for research use only and is not intended for therapeutic or diagnostic applications. Please contact a technical service representative for more information. All products of animal origin manufactured by Rockland Immunochemicals are derived from starting materials of North American origin. Collection was performed in United States Department of Agriculture (USDA) inspected facilities and all materials have been inspected and certified to be free of disease and suitable for exportation. All properties listed are typical characteristics and are not specifications. All suggestions and data are offered in good faith but without guarantee as conditions and methods of use of our products are beyond our control. All claims must be made within 30 days following the date of delivery. The prospective user must determine the suitability of our materials before adopting them on a commercial scale. Suggested uses of our products are not recommendations to use our products in violation of any patent or as a license under any patent of Rockland Immunochemicals, Inc. If you require a commercial license to use this material and do not have one, then return this material, unopened to: Rockland Inc., P.O. BOX 5199, Limerick, Pennsylvania, USA.